



Stability and selectivity of pre-concentration methods for gaseous oxidized mercury in the air

Sreekanth Vijayakumaran Nair^{1,2}, Saeed Waqar Ali^{1,2}, Jan Gačnik^{1,2}, Igor Živković^{1,2}, Teodor-Daniel Andron^{1,2}, Oleg Travnikov¹, Milena Horvat^{1,2}

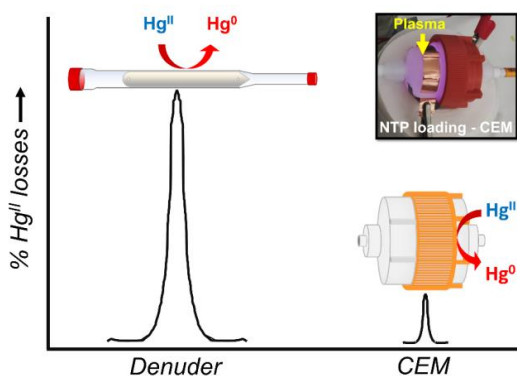
¹Department of Environmental Sciences, Jožef Stefan Institute, Ljubljana, Slovenia

²Jožef Stefan International Postgraduate School, Ljubljana, Slovenia

Correspondence to: Milena Horvat (milena.horvat@ijs.si)

Abstract. The determination of gaseous oxidized mercury (GOM, Hg^{II}) in the atmosphere at ultra-trace levels necessitates a preconcentration step. KCl-coated denuders and cation exchange membranes (CEMs) are widely used preconcentration methods for sampling Hg^{II} . Sampling losses during preconcentration could result in measurement biases. This study evaluated the performance of denuders and CEMs in retaining Hg^{II} , to accurately estimate biases through a precise mass balance approach using ^{197}Hg radiotracer and generation of specific Hg^{II} species by non-thermal plasma oxidation of Hg^0 in the presence of reactant gases. The results showed that recovery of Hg^{II} by thermal decomposition from freshly prepared denuders were approximately 100%. The retention of Hg^{II} on denuders during sampling period was much poorer compared to CEMs. Freshly prepared denuders lost up to 61.5% of Hg^{II} , while reused denuders lost up to 79.7% after 2 hours of ambient air exposure. CEMs exhibited much lower losses over 72 hours: on average, 16.7% for HgO , 2.7% for HgCl_2 , and 3.8% for HgBr_2 . The standard digestion procedure for CEMs by BrCl digestion was found to be incomplete, with a few residual amounts detected on CEMs post-digestion (5.3% on average). Additionally, the overall mass distribution within the CEM filter pack cartridges revealed that some Hg^{II} was retained on their inner Teflon parts. These findings underscore the critical importance of addressing biases in methods adopted for Hg^{II} measurements, to improve the accuracy and reliability of atmospheric Hg data, an integral component in evaluating Hg model outputs for Minamata convention effectiveness evaluation.

Graphical abstract.





25

1 Introduction

Mercury (Hg) is a volatile toxic element globally distributed in atmospheric, terrestrial, and aquatic environments. Hg is emitted into the atmosphere from various natural and anthropogenic sources (Kocman et al., 2013; Outridge et al., 2018; Pacyna et al., 2006; Peter Mason et al., 2024; Pirrone et al., 2009; Selin, 2009). Once emitted into the atmosphere, Hg undergoes complex chemical transformations, regional and global transport, dry and wet deposition to terrestrial and aquatic environments, and remission (Driscoll et al., 2013; Gonzalez-Raymat et al., 2017; Lyman et al., 2020a; Ryaboshapko et al., 2002; Xu et al., 2013; Zhang et al., 2012). Atmospheric Hg commonly exists in 0 and +2 oxidation states (Schroeder and Munthe, 1998; Si and Ariya, 2018). However, based on sampling protocols, they are operationally defined as gaseous elemental Hg (GEM, Hg^0), gaseous oxidized Hg (GOM, Hg^{II}), and particulate-bound Hg (PBM, PHg^{II}) (Ariya et al., 2015; Gustin et al., 2015; Zhang et al., 2021).

Measurement of oxidized Hg fractions is quite challenging due to their high chemical reactivity and ultra-trace level presence in the ambient air. The exact chemical composition of Hg^{II} is not precisely known in real-time and Hg^{II} species are collectively sampled and reported as GOM fraction (Gustin and Jaffe, 2010; Huang et al., 2017). For the past few decades, atmospheric Hg^{II} measurements have mostly been performed using commercially available Tekran 2537/1130 unit, based on preconcentrating Hg^{II} (1-2 hours) on KCl-coated denuders followed by thermal decomposition and subsequent detection as Hg^0 by the means of cold vapor atomic fluorescence spectrometry (CVAFS) (Landis et al., 2002). Alternatively, cation exchange membranes (CEMs) are used as a preconcentration media, specifically for Hg^{II} or reactive mercury (RM: $\text{Hg}^{\text{II}}+\text{PHg}^{\text{II}}$), where the sampling period generally lasts from 1 to 2 weeks. Post-sampling recovery of Hg^{II} from the CEM for analysis is based on overnight digestion in BrCl solution and detection is commonly performed by CVAFS (Gustin et al., 2019; Luippold et al., 2020; Miller et al., 2019).

The primary pathway of delivery of Hg from atmosphere to terrestrial and aquatic environments is the oxidation of Hg^0 to Hg^{II} and subsequent deposition processes (Jaffe et al., 2014). Hg^{II} thus offers a crucial connection between anthropogenic Hg emissions and ecological exposure. Current models predicting Hg distribution and deposition suffer from biased low Hg^{II} measurements (Cheng and Zhang, 2017; Dastoor et al., 2022; Travníkov et al., 2017). These biases arise from two primary sources. Firstly, insufficient information on emission sources hinders accurate modeling due to the lack of detailed knowledge about the specific Hg species being emitted, and secondly, measurement biases leading to significant underestimation of Hg^{II} concentrations. Measurement biases originate from both calibration and sampling methods (Davis and Lu, 2022). Traditional methods, such as using KCl-coated denuders or CEMs, have shown significant discrepancies in measured Hg^{II} concentrations. These methods were previously reported to suffer from biases and interferences from humidity and ozone (Dunham-Cheatham et al., 2023; Gustin et al., 2019; Huang et al., 2013; Huang and Gustin, 2015; Lyman et al., 2010; McClure et al., 2014). Such measurement biases, driven by the high reactivity and chemical nature of Hg^{II} , lead to significant underestimation of ambient air Hg^{II} concentrations. This results in inaccuracies in model outputs, potentially affecting our understanding of Hg transport, transformation, and deposition processes in the atmosphere. Therefore, accurate Hg^{II} measurements are vital for understanding and modeling Hg deposition patterns, and for the effectiveness evaluation of Minamata convention (UNEP, 2021).

Most measurements of Hg^{II} , including those made with CEMs, lack proper calibration to the SI traceability, thus making it difficult to assess their validity. A few groups have investigated methods to quantitatively calibrate Hg^{II} measurements, and progress is noticeable in recent years (Dunham-Cheatham et al., 2023; Feng et al., 2003; Gačnik et al., 2021b, 2022a; Lyman et al., 2016, 2020b; Sari et al., 2020; Vijayakumaran Nair et al., 2024). A recent review assessed that permeation tube-based systems are



currently the best candidate for calibrating ambient Hg^{II} measurements in field settings, as they provide a continuous traceable quantity of Hg^{II} (Gustin et al., 2024). Moreover, the calibration approach using cold plasma for quantitative oxidation of traceable Hg^0 vapor has shown great promise as well (Gačnik et al., 2022a; Vijayakumaran Nair et al., 2024). Both methods were compared in a recent study (Elgiar et al., 2024).

Recent recommendations have highlighted the need for improved Hg^{II} measurement techniques to address these biases (Gustin et al., 2024). These recommendations emphasized developing methods that minimize calibration and sampling errors to enhance the accuracy of atmospheric Hg models. Based on that, this study aims to address the critical issue of biased low Hg^{II} measurements. Unlike previous studies that relied on sublimation sources (permeation tubes) for the stable production of Hg^{II} , our approach utilized non-thermal plasma (NTP) oxidation of Hg^0 for controlled generation of various Hg^{II} species (Gačnik et al., 2022b; Vijayakumaran Nair et al., 2024). This approach helps validate how the methods behave to different Hg^{II} species, as the plasma source provides a unique opportunity to study different Hg^{II} species generated using a single calibration source. The application of Hg radiotracer (^{197}Hg) further enhances experimental precision by eliminating concerns regarding blanks and contamination. Laboratory experiments, implemented at environmentally relevant concentrations, utilized the ^{197}Hg to provide a precise mass balance budget, enabling accurate quantification of biases in Hg^{II} measurement methods.

The primary objective of this study was to quantify biases occurring from pre-concentration methods commonly used for sampling Hg^{II} in air. This includes the evaluation of the performance of KCl-coated denuders and CEMs at retaining Hg^{II} species during pre-concentration when exposed to ambient air. The goals of this work were to perform laboratory experiments to i) evaluate denuder performance for Hg^{II} retention during pre-concentration, ii) quantify Hg^{II} losses from CEM during the pre-concentration period, and iii) assess Hg^{II} recovery efficiency from denuders and CEMs.

2 Materials and methods

2.1 Production of ^{197}Hg radiotracer

The production of ^{197}Hg radiotracer was previously described elsewhere (Ali et al., 2024; Gačnik et al., 2021b, 2022b). Hg stock solution enriched to 51.58% in ^{196}Hg isotope (0.15% natural abundance) was used for the production of ^{197}Hg radiotracer. The sealed ampoule filled with enriched ^{196}Hg stock was irradiated in a strong neutron flux for 12 hours in the central channel of the 250 kW TRIGA Mark II research reactor at the Jožef Stefan Institute in Slovenia. This results in the formation of ^{197}Hg ($t_{1/2} = 2.671$ days) based on a neutron capture reaction (n, γ). Irradiated ampoule was carefully opened, and the solution was transferred in separate vial for storage. Intermediate working standard solutions in 5% v/v HNO_3 were prepared from the main irradiated stock solution ($^{197}\text{Hg}^{2+}$) with the concentration $100 \mu\text{g mL}^{-1}$. The concentration of stock solution was previously determined by using CV-AAS (Model HG-201 semi-automated Hg analyzer) calibrated against NIST SRM 3133.

2.2 Loading denuder and CEM with Hg^{II}

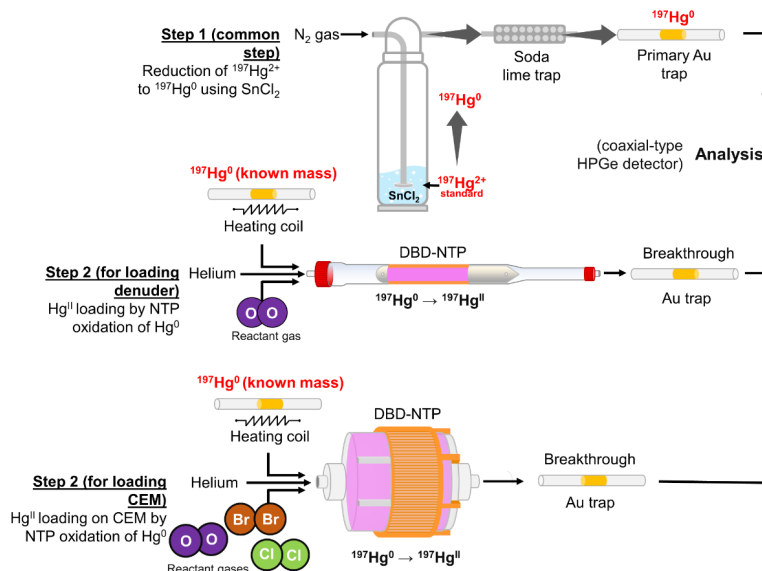


Figure 1: Schematic representation of steps involved in loading KCl-coated denuders and CEMs with known amount of Hg^{II} by NTP-assisted oxidation of Hg^0 vapour. Reactant gases used were O_2 , Cl_2 , and Br_2 , to generate oxidized species HgO , HgCl_2 , and HgBr_2 , respectively.

The detailed procedure for coating denuders with KCl was previously described (Landis et al., 2002; Vijayakumaran Nair et al., 2024). Loading denuders and CEMs with $^{197}\text{Hg}^{\text{II}}$ was performed in two steps (Figure 1). The amount of ^{197}Hg used for loading denuders ranged between 250 pg to 6.2 ng, while experiments on CEMs were conducted using ^{197}Hg standards ranging from 2.5 ng to 30 ng. The first step involved the complete chemical reduction of known concentrations of Hg ($^{197}\text{Hg}^{2+}$ radiotracer) standard solution spiked in an impinger continuously purged with N_2 at a flowrate of 1400 mL min^{-1} in the presence of 5 mL SnCl_2 solution (10% SnCl_2 (w/v) prepared in 10% HCl (v/v)). $^{197}\text{Hg}^{2+}$ ions in solution reduced by SnCl_2 to $^{197}\text{Hg}^0$ vapor was trapped in a primary gold (Au) trap through amalgamation after drying in a soda lime trap kept upstream of the Au trap. This primary Au trap with known amount of $^{197}\text{Hg}^0$ (measured in a coaxial type HPGe detector) was then used in the second step for loading denuders and CEMs by NTP-assisted oxidation of Hg^0 to generate Hg^{II} . Here, O_2 directly obtained from a gas cylinder (99.999% purity) was used as the reactant gas to produce HgO for loading denuders. Experiments were performed using dielectric barrier discharge (DBD)-NTP generated by applying high voltage to a pair of copper strips (acting as electrodes) attached on the denuder surface (quartz tube acting as a dielectric barrier). A pair of copper electrodes, 1 mm in thickness, 12 mm wide, and 135 mm in length, were attached on opposite sides of the collection area of the denuder. Upon igniting the NTP, the primary Au trap was heated to approximately 400°C to release Hg^0 , which was transferred into the plasma via primary tubing, while the reactant gas was introduced through secondary tubing. Helium gas was utilized both to generate plasma and as the carrier gas for Hg^0 and reactant gases. NTP generated $^{197}\text{Hg}^{\text{II}}$ was retained on the denuder whereas breakthrough ($^{197}\text{Hg}^0$) was captured in a secondary Au trap kept downstream of the denuder outlet.

Reactant gases used for loading CEMs were O_2 , Cl_2 , and Br_2 . The Cl_2 gas was produced in the laboratory based on the reaction between calcium hypochlorite with HCl , whereas Br_2 gas was generated from the reaction between hydrobromic acid and N-bromosuccinimide. The method used for the production of Cl_2 and Br_2 gas in this study was different from previous studies, (Gačnik et al., 2022a; Vijayakumaran Nair et al., 2024) as the present method was less time-consuming, more efficient, and had better



reproducibility. CEMs (Pall Corporation - Mustang MSTGS3R) cut off into standard diameter (47 mm) was used for all experiments. The CEM filter pack cartridge was used both as a dielectric barrier for plasma generation and a reactor vessel for NTP oxidation of $^{197}\text{Hg}^0$ to $^{197}\text{Hg}^{\text{II}}$. A pair of copper electrode was attached around the outer surface of the CEM filter pack, leaving behind approximately 20 mm gap between both electrodes.

To check the efficiency of NTP oxidation for loading CEM with $^{197}\text{Hg}^{\text{II}}$, mass balance was checked by taking into consideration of the breakthrough during loading, CEM digestate for $^{197}\text{Hg}^{\text{II}}$, CEM leftover for any residual $^{197}\text{Hg}^{\text{II}}$ post-digestion, and $^{197}\text{Hg}^{\text{II}}$ attached to the inner Teflon parts of the filter pack cartridge by acid-washing. For denuders, mass balance was checked by considering breakthrough during loading and $^{197}\text{Hg}^{\text{II}}$ retained on the denuder (measured by thermal decomposition and collection on an Au trap).

2.3 Quantification of Hg^{II} losses from denuders and CEM

The activity of ^{197}Hg was measured either using a well-type or coaxial-type HPGe detector depending on the sample collection matrix. ^{197}Hg activity on Au traps and KCl traps were measured in the coaxial-type HPGe detector whereas solutions in the well-type HPGe detector. Information on the determination of ^{197}Hg activity (both samples and standards) using an HPGe detector was previously described (Ali et al., 2024; Gačnik et al., 2021b, a, 2022b; Ribeiro Guevara et al., 2007). Peak area comparison of the sample and standard activity for the characteristic doublet peaks of γ -ray and X-ray emissions ($67.0 + 68.8$ and $77.3 + 78.1$ keV) was performed using Genie 2000 Gamma analysis software. To account for measurements made at different times, the peak areas of samples and standard activities were corrected for nuclear decay relative to a reference time, defined as the start of the experiment (Ribeiro Guevara et al., 2007). Standards for solid samples (Au traps) were prepared the same way described above (section 2.2) for loading primary Au trap. For well-type detector, standards were prepared in triplicates by spiking radiolabeled solution (desired concentrations) into MQ with 5% HNO_3 (v/v) for desired concentrations. 8 mL of each standards were transferred into separate vials for measurements in the well-type HPGe detector similar to the analysis of all sample solutions.

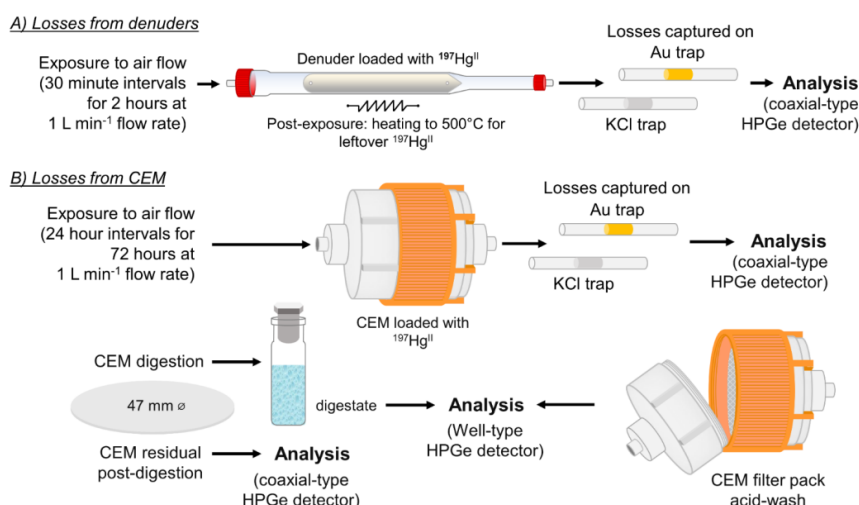


Figure 2: Quantification of Hg^{II} losses from A) denuders and B) CEM, pre-loaded with known amount of $^{197}\text{Hg}^{\text{II}}$, exposed to ambient air flow. Au trap was used to capture Hg^{II} losses in reduced form (Hg^0), while a KCl trap was kept upstream of the Au trap to capture losses in the form of Hg^{II} . Mass balance was determined at the end of each experiment.



The quantification of losses $^{197}\text{Hg}^{\text{II}}$ from the denuder was based on the exposure of KCl-coated denuders loaded with known amounts of ^{197}HgO to different airflows under dark and light conditions. Denuders were exposed to ambient air and N_2 flow for 2 hours at 1 L min^{-1} flow rate with losses measured every 30 minutes. Denuders were exposed to light and dark conditions to examine the influence of light on sampling losses from denuders. As air was pulled through denuder inlet, an Au trap was placed on the other end of the denuder to capture losses for quantification. A KCl-trap was also plugged before the Au trap to check whether the losses are in the form of Hg^{II} or Hg^0 (Gačnik et al., 2021a). Losses were quantified by measuring the activity of ^{197}Hg collected on Au traps and KCl traps in a coaxial-type HPGe detector. Measured activity was then compared with the known activity of the standard used for initially loading the denuder.

In contrast to denuders, CEMs loaded with $^{197}\text{Hg}^{\text{II}}$ (HgO , HgCl_2 , HgBr_2) were exposed to ambient air flow for longer duration (72 hours) to imitate the common sampling procedure when using CEMs (Gustin et al., 2019). Pumps were used to draw ambient air through the CEM filter pack at the flow rate of 1 L min^{-1} . Au traps were used to collect ^{197}Hg losses from the CEM. A KCl trap was also used to capture any losses in the form of Hg^{II} itself. Losses were quantified by measuring those Au and KCl traps in a coaxial-type HPGe detector. For the determination of complete mass balance, CEMs after the whole exposure period was digested overnight in BrCl solution following the standard procedure described elsewhere (Gustin et al., 2019). From the digestate, 8 mL was used for quantification in a well-type HPGe detector. Following the CEM digestion, each CEMs were rinsed thoroughly with MQ water, dried, and analyzed for any leftovers in the Coaxial type HPGe detector. The Filter pack cartridges were leached with 15 mL of acid washing solution (10% HNO_3 : 5% HCl v/v) to quantify $^{197}\text{Hg}^{\text{II}}$ remaining on their inner Teflon parts. Similar to denuders, Au traps and KCl traps were compared with the activity of Au trap standard. Meanwhile, ^{197}Hg activity in sample solutions were compared with their corresponding standards prepared for well-type HPGe detector described above.

2.4 Data analysis

Data analyses and visualizations were performed using SigmaPlot v14.0. Comparisons between two variables were made using paired t-tests, while for comparisons involving more than two variables, one-way ANOVA was employed. Pearson's correlation test was used to assess the relationship between variables. All statistical tests were conducted at a 95% confidence interval.

3 Results and discussion

3.1 NTP loading and recovery efficiency

The NTP oxidation efficiency for loading denuders with $^{197}\text{Hg}^{\text{II}}$ is shown in Figure 3. In general, NTP loading efficiency ranged between 86.2–96.1%, with an average efficiency of 94.2% ($\pm 1.9\%$ SD, $n=3$), 88.7% ($\pm 1.6\%$ SD, $n=3$), 89.5% ($\pm 3.5\%$ SD, $n=3$) for denuders A, B, and C respectively. Differences in the loading efficiency between the denuders were not statistically significant ($P = 0.072$). The breakthrough during loadings were averaged at 6.5% ($\pm 2.3\%$ SD, $n=3$), 10.6% ($\pm 1.3\%$ SD, $n=3$), and 10.4% ($\pm 2.1\%$ SD, $n=3$) for denuders A, B, and C respectively. To obtain a quantitative mass balance, in addition to breakthroughs, plasma GOM ($^{197}\text{Hg}^{\text{II}}$) loaded on denuders was recovered by heating denuders in a portable oven unit (Lindberg/Blue M Tube Furnace, Model Number: TF55030C-1) at 500°C for 15 minutes under the stream of N_2 gas and collected on Au traps kept downstream of denuders. The average Hg^{II} recovery efficiency from denuders by thermal decomposition was 101% ($\pm 2.1\%$ SD, $n=9$).

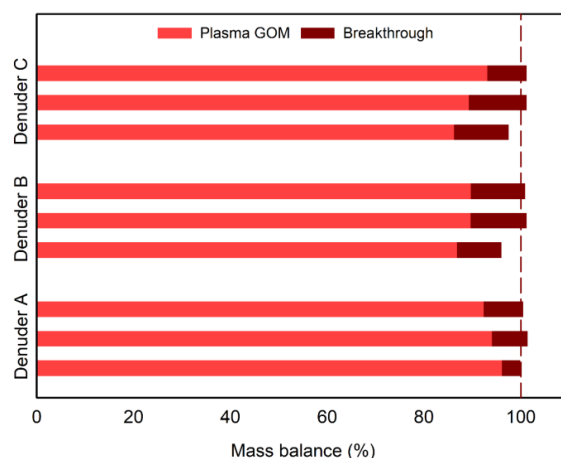


Figure 3: Mass balance for plasma oxidation of $^{197}\text{Hg}^0$ to $^{197}\text{Hg}^{\text{II}}$ performed on denuders. “Plasma GOM” refers to $^{197}\text{Hg}^{\text{II}}$ retained on denuders, generated by the NTP oxidation method whereas “Breakthrough” refers to unoxidized $^{197}\text{Hg}^0$ collected on the breakthrough Au trap.

The NTP oxidation efficiencies for loading CEMs with different Hg^{II} species (HgO , HgCl_2 , and HgBr_2) are illustrated in Figure 4.

The NTP oxidation efficiency for generating Hg^{II} within the CEM filter pack (as a dielectric barrier reactor vessel) ranged from 90.2–102% for HgO , 94.2–98.0% for HgCl_2 , and 92.2–98.2% for HgBr_2 . The average breakthrough was below 1% for HgCl_2 and HgBr_2 , while for HgO , it was 4.6% ($\pm 1.7\%$ SD, $n=5$). Regarding the overall mass balance during $^{197}\text{Hg}^{\text{II}}$ loading, the average Hg^{II} collected on CEMs was 87.3% ($\pm 5.6\%$ SD, $n=5$) for HgO , 92.9% ($\pm 2.4\%$ SD, $n=6$) for HgCl_2 , and 87.4% ($\pm 7.0\%$ SD, $n=6$) for HgBr_2 . Meanwhile, an average of 6.5% ($\pm 1.8\%$ SD, $n=5$), 4.3% ($\pm 3.0\%$ SD, $n=6$), and 7.7% ($\pm 5.6\%$ SD, $n=6$) Hg^{II} was retained on the inner Teflon walls of the filter pack for HgO , HgCl_2 , and HgBr_2 , respectively.

The mass balance analysis revealed that not all Hg^{II} generated by NTP within the filter pack cartridge was collected on CEMs, but a considerable amount was distributed on the inner Teflon surface of the filter pack cartridges. This distribution pattern was similar for all Hg^{II} species studied. When considering the percentage of total Hg^{II} generated by NTP within the filter pack cartridges (excluding breakthroughs), an average of 93.0% of the total generated HgO was collected on the CEM, while the remaining 7.0% was collected on the inner Teflon components of the filter pack cartridge. For HgCl_2 , the respective retentions were 95.6% and 3.6%, and for HgBr_2 , they were 94.1% and 5.9%, respectively. Following this, the recovery of Hg^{II} from CEMs through BrCl digestion ranged from 92.1% to 97.1% for all Hg^{II} species, with average recoveries of 94.8% ($\pm 2.1\%$ SD, $n=5$), 94.0% ($\pm 1.7\%$ SD, $n=6$), and 93.5% ($\pm 0.7\%$ SD, $n=6$) for HgO , HgCl_2 , and HgBr_2 , respectively. Post-digestion measurements on digested CEM revealed that CEMs retained a small fraction of Hg^{II} as residuals, averaging 5.5% ($\pm 2.4\%$ SD, $n=5$), 6.4% ($\pm 2.0\%$ SD, $n=6$), and 6.9% ($\pm 0.8\%$ SD, $n=6$) for HgO , HgCl_2 , and HgBr_2 , respectively. Discussions on implication of Hg^{II} recovery as digestion leftover residuals and from Teflon parts are discussed later.

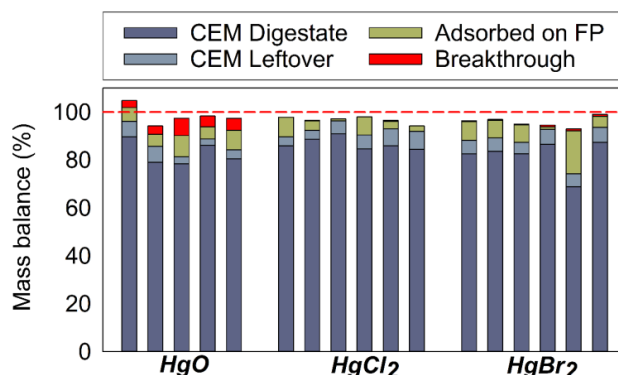


Figure 4: Plasma oxidation of Hg^0 to Hg^{II} performed on CEMs for the production of HgO , HgCl_2 , and HgBr_2 . Overall mass balances for NTP- Hg^{II} loading are represented here, as the sum of Hg^{II} recovered from CEMs by digestion, residual leftover in CEMs post-digestion, Hg^{II} recovered from the inner Teflon walls of the filter pack (FP) cartridge, and breakthrough collected on the Au trap during loading.

3.2 Sample (Hg^{II}) losses during preconcentration

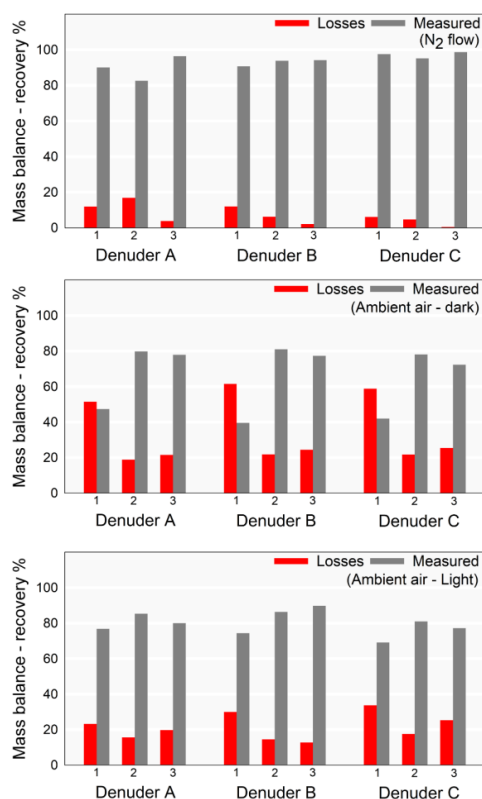


Figure 5: Denuder stability (Hg^{II} sample losses) at different conditions when exposed to various airflows. Mass balances are shown here as sum of $^{197}\text{Hg}^{\text{II}}$ losses quantified at each exposure period (4×0.5 hours), based on the initially loaded $^{197}\text{Hg}^{\text{II}}$ on the denuders, and the $^{197}\text{Hg}^{\text{II}}$ finally recovered from the denuders at the end of the exposure period through thermal decomposition, referred to as the "Measured" fraction.



Efficiency of Hg^{II} retention on freshly prepared denuders under various conditions is summarized in Figure 5, along with the corresponding mass balances obtained after the exposure period. Detailed information on losses measured at each exposure interval is provided in Table S3 in the supplementary material. Our findings from this study for denuders are similar to those losses reported by Lyman et al. (2010) for Hg halides (29–55%). The mass balance from these experiments indicates good recoveries of remaining Hg^{II} from denuders after the exposure period to ambient air, with the average mass balance quantified at 100.7% ($\pm 1.8\%$ SD, $n = 18$). The average Hg^{II} losses from denuders were observed to be minimal when exposed to N_2 flow ($7.1 \pm 5.3\%$ SD, $n=9$), where maximum losses were observed within the first half hour of the exposure period (Table S3 in the supplementary material). In contrast to the N_2 flow, denuders exhibited poor Hg^{II} retention when exposed to the ambient air flow, both in dark and light conditions. Cumulative Hg^{II} losses from denuders averaged 33.9% ($\pm 17.8\%$ SD, $n = 9$) under dark conditions, with a maximum loss of 61.5%, while under ambient light, losses averaged 21.4% ($\pm 7.2\%$ SD, $n = 9$) with a maximum of 33.7%. There was no statistically significant difference in Hg^{II} losses observed between denuders A, B, and C ($p > 0.05$). Although the differences in Hg^{II} losses between light and dark conditions are not clearly understood, they have been attributed to variations in relative humidity (RH%), supported by a strong positive correlation between Hg^{II} losses and RH ($R_{\text{corr}} = 0.977$; $P < 0.001$). Depending on the RH levels in the ambient air during exposure periods, denuders retained only between 39.5% and 89.8% of the initially loaded Hg^{II} . Throughout these experiments, no observable ^{197}Hg activity was detected on KCl traps placed downstream of denuders, indicating that all Hg^{II} losses captured on Au traps from denuders were in the form of Hg^0 (GEM).

Studies have previously reported that the performance of KCl-coated denuders for measuring Hg^{II} is significantly affected by humidity (Huang et al., 2013; Huang and Gustin, 2015; McClure et al., 2014). Huang and Gustin (2015) have shown that the efficiency for Hg^{II} collection on KCl-coated denuders can decline by 4–60% during spikes of relative humidity (25 to 75%) (Huang and Gustin, 2015). The reason for this loss of Hg^{II} in KCl denuders under high humidity conditions is that the moisture can hydrolyze the KCl-coated surface. This creates another layer for compounds to be transported from air to the collection surface, potentially reducing the capture efficiency (Huang et al., 2013). Additionally, it has been suggested that under high-humidity conditions, Hg^{II} can be converted to GEM or detected as such (Gačnik et al., 2021a; McClure et al., 2014). In some cases, the KCl-coated denuders were gradually passivated over time after additional humidity was applied (Huang and Gustin, 2015). In the present study, while freshly prepared denuders lost upto 61.5% initially loaded Hg^{II} , re-used denuders that have previously exposed to ambient air and undergone several heating cycles exhibited even poorer Hg^{II} retention capabilities (Supplementary material – Table S4). Those denuders exhibited much higher Hg^{II} losses, upto 79.7%, with an average loss of 51.0% ($\pm 18.6\%$ SD, $n=20$).

Table 1: $^{197}\text{Hg}^{\text{II}}$ losses from CEM loaded with different $^{197}\text{Hg}^{\text{II}}$ species (HgO , HgCl_2 , and HgBr_2) when exposed to ambient air flow for a total exposure period of 72 hours. Losses were measured every 24 hours, and their sum is represented here as a percentage of the actual amount of $^{197}\text{Hg}^{\text{II}}$ initially loaded on CEMs.

<i>Hg^{II} losses from CEM (72 hours): HgO loaded on CEM</i>						
Amount (ng)	CEM	Losses (%)	CEM Digestate (%)	CEM Leftover (%)	FP wash (%)	Mass balance (%)
2.5	A	20.3	65.8	5.8	2.9	94.8
2.5	B	18.7	63.2	9.6	2.2	93.7
60	C	13.8	65.3	7.0	9.9	96.0
10	A	18.8	76.4	4.8	0.3	100.4
10	B	15.7	75.0	6.2	2.6	99.5
10	C	20.3	71.9	6.0	1.4	99.7
30	A	12.9	78.7	5.4	1.0	98.0
30	B	15.4	70.3	5.3	8.9	100.0
30	C	14.8	66.4	8.6	8.7	98.5
Average		16.7	70.3	6.5	4.2	97.8



<i>Hg^{II} losses from CEM (72 hours): HgCl₂ loaded on CEM</i>						
Amount	CEM	Losses	CEM Digestate	CEM Leftover	FP wash	Mass balance
2.5	A	3.0	85.5	4.4	2.8	95.7
2.5	B	2.4	87.5	4.9	3.1	97.8
2.5	C	4.0	85.2	7.5	3.0	99.7
10	A	2.3	87.2	4.7	0.6	94.9
10	B	2.7	87.9	5.3	0.5	96.4
10	C	4.0	86.6	1.9	6.3	98.8
30	A	2.6	94.1	4.8	0.4	101.9
30	B	2.4	88.8	4.8	0.7	96.7
30	C	1.3	88.9	5.5	2.6	98.3
Average		2.7	88.0	4.9	2.2	97.8
<i>Hg^{II} losses from CEM (72 hours): HgBr₂ loaded on CEM</i>						
Amount	CEM	Losses	CEM Digestate	CEM Leftover	FP wash	Mass balance
2.5	A	3.7	93.1	3.6	0.4	100.8
2.5	B	1.1	91.8	5.4	2.3	100.5
2.5	C	4.5	92.4	5.1	0.2	102.3
10	A	5.2	84.8	3.3	4.9	98.2
10	B	5.6	85.5	4.2	3.4	98.7
10	C	4.8	88.4	4.5	2.6	100.2
30	A	3.7	93.1	3.6	0.4	100.8
30	B	1.1	91.8	5.4	2.3	100.5
30	C	4.5	92.4	5.1	0.2	102.3
Average		3.8	90.4	4.5	1.9	100.5

The findings of tests on CEMs exposed to ambient air is summarized in Table 1. Overall mass balances observed for total Hg^{II} recovery of initially loaded Hg^{II} on CEMs were on average 97.8% ($\pm 2.4\%$ SD, n=9) of HgO, 97.8% ($\pm 2.2\%$, n=9) for HgCl₂, and 100.5% ($\pm 1.4\%$, n=9) for HgBr₂. For HgO, average of total sample losses from CEM was quantified at 16.7% ($\pm 2.8\%$ SD, n=9). In contrast to denuders, ¹⁹⁷Hg activity was detected in KCl traps kept downstream between CEM and Au trap, indicating partial losses in the form of Hg^{II}, averaged at 2.7% ($\pm 2.4\%$ SD, n=9). This could be due to weak retention of HgO on the inner Teflon parts of the filter pack cartridge. To confirm this, freshly loaded CEMs were transferred to clean filter pack cartridges to check whether there were losses from CEMs in the form of Hg^{II}. However, in these cases, there was no ¹⁹⁷Hg activity detected in the KCl traps, indicating poor retention of HgO on the inner Teflon parts of the filter pack cartridge. In contrast to HgO, losses of HgCl₂ and HgBr₂ from CEMs were very minimal, averaging at 2.7% ($\pm 0.8\%$ SD, n=9) and 3.8% ($\pm 1.7\%$ SD, n=9) respectively. The average amount of Hg^{II} lost from the filter pack cartridge in its original form (Hg^{II}) was negligible, <0.1% for HgCl₂ and HgBr₂ were detected in KCl traps. The Hg^{II} losses were negatively correlated with initial concentration of Hg^{II} loaded on CEMs for HgO ($R_{\text{corr}} = -0.78$; $P = 0.0123$), but with no statistical significance for negative correlation observed for HgCl₂ and HgBr₂ ($P > 0.050$). No statistically significant difference was observed between the losses quantified for HgCl₂ and HgBr₂. However, both HgCl₂ and HgBr₂ exhibited notable difference from losses observed for HgO, statistically significant at $P < 0.050$. Compared to HgCl₂ and HgBr₂, the higher losses observed for HgO (upto 20.3%) from membranes could be due to weak bonding of HgO (a basic oxide) on CEM surface. Meanwhile, HgCl₂ and HgBr₂ are Lewis acids (Sandström et al., 1990) which are strongly bonded with CEM surface, thus exhibits very high retention of these compounds.

After 72 hours of exposure to ambient air, 81.0% ($\pm 4.0\%$ SD, n=9) of the initially loaded HgO remained in the CEM setup, with a maximum retention of 85.1%. Of this remaining Hg^{II}, 70.3% ($\pm 5.5\%$ SD, n=9) was recovered in the BrCl digestate, 4.2% ($\pm 3.8\%$ SD, n=9) from the inner Teflon surface of the filter pack cartridge, and 6.5% ($\pm 1.6\%$ SD, n=9) was retained as post-digestion Hg^{II} residuals on the CEMs. In contrast, HgCl₂ and HgBr₂ showed maximum retentions of 99.3% and 99.5%, respectively, with



260 average retentions of 95.1% ($\pm 2.1\%$ SD, $n=9$) for HgCl_2 and 96.8% ($\pm 2.4\%$ SD, $n=9$) for HgBr_2 . From these, 88.0% ($\pm 2.6\%$ SD, $n=9$) of HgCl_2 and 90.4% ($\pm 3.3\%$ SD, $n=9$) of HgBr_2 were measured in the BrCl digestate, while residuals on CEMs were quantified at 4.9% ($\pm 1.4\%$ SD, $n=9$) for HgCl_2 and 4.5% ($\pm 0.8\%$ SD, $n=9$) for HgBr_2 . Post-digestion residuals on CEMs showed no significant correlation with the initial concentrations of Hg^{II} loaded, but HgO residuals differed significantly ($P < 0.050$) compared to those of HgCl_2 and HgBr_2 . The remaining HgCl_2 ($2.2\% \pm 1.9\%$ SD, $n=9$) and HgBr_2 ($1.9\% \pm 1.7\%$ SD, $n=9$) were
 265 recovered from the inner Teflon parts of the filter pack cartridges. Gačnik et al. (2021b) previously estimated the adsorption enthalpy of HgCl_2 on Teflon surface ($\Delta H_{\text{ads}} = -12.33 \text{ kJ mol}^{-1}$), thus showing that the binding of mercury halogenides to Teflon is energetically favorable and is especially significant at lower temperatures.

The presence of post-digestion Hg^{II} residuals on CEMs indicates incomplete digestion with the BrCl method. While the residual amounts were minimal, we attempted their recovery through overnight leaching with tetrabutylammonium solution, which is
 270 commonly used for aqueous biphasic extraction of metal ions (Smirnova et al., 2021). This approach resulted in an additional (upto 3.5%) recovery, but residual traces were still detected on the leached CEM surfaces. In a further preliminary attempt to recover residuals on CEM, we employed microwave digestion using strong acids (as described in Supplementary Material S5 and Table S6). This approach successfully improved Hg^{II} recovery from CEMs upto 100.4% ($\pm 0.4\%$ SD, $n=3$). Further investigation is required in future studies to assess its robustness and potential as a viable alternative to BrCl digestion method for Hg^{II} recovery
 275 from CEMs. Discussions from the paper on the current limitations and suggestions for atmospheric Hg measurements also emphasized the need to develop new methods to enhance the accuracy of Hg^{II} measurements (Gustin et al., 2024).

The study highlights the limitations of both denuder and CEM methods in accurately measuring Hg^{II} as it is evident that these methods do not retain all the loaded Hg^{II} equally. However, CEM has demonstrated better retention of Hg^{II} species and stands out as a more reliable alternative to KCl denuders for Hg^{II} measurements. Previous studies have reported that CEM systems measured
 280 higher levels of Hg^{II} compared to KCl denuders when both were used simultaneously. Upon comparing the uptake of specific Hg^{II} compounds by denuders, nylon membranes, and CEMs, Huang et al. (2013) reported different affinities for Hg^{II} compounds on the denuder surface. Additionally, their findings revealed large disparities between Hg^{II} measurements obtained by membranes and denuders. Membrane-based measurements were reported to be from 1.3 to 3.7 times higher than denuder-based measurements, both in field and laboratory experiments. Gustin et al. (2019) reported that RM measurements from the RMAS 2.0 (Reno-Reactive
 285 Mercury Active Systems) were 3.7 times higher than those from the Tekran 2537/1130 system. Additionally, Tekran 1130 Hg^{II} measurements were correlated with Hg^{II} data from the CEM in the RMAS+PTFE system. These findings indicate that while both systems measure similar Hg^{II} /RM concentrations, the values differ significantly in magnitude. It was suggested that if seasonal RMAS data is available for a particular sampling location, it could be used to correct Hg^{II} values obtained from the Tekran system for improved accuracy (Gustin et al., 2019). A similar approach was proposed by Maruszczak et al. (2017) to apply bias corrections
 290 to Tekran-based RM and Hg^{II} data. Their corrected dataset from Pic du Midi (2012–2014) showed that Hg^{II} and RM levels showed strong agreement with both in-flight RM observations and model-based Hg^{II} & RM estimates, highlighting the effectiveness of such corrections in improving measurement accuracy (Maruszczak et al., 2017). Additionally, Travníkov et al. (2024), highlighted the importance of RM measurements for understanding atmospheric mercury processes and improving chemical transport models, particularly for evaluating the Minamata Convention's effectiveness. They suggest that using historical RM observations with
 295 corrected biases, caused by inaccuracies in KCl-coated denuder technology, for model evaluation can help identify additional uncertainties, such as speciation of Hg anthropogenic emissions and near-ground RM redox and deposition processes, and improve model estimates of mercury atmospheric transport and deposition to ecosystems (EMEP, 2024).



4 Conclusions

This study systematically evaluated the performance of KCl-coated denuders and CEMs for the preconcentration of Hg^{II} in atmospheric measurements. Our findings highlight the significant biases associated with current measurement methods, emphasizing the need for improvements to ensure accurate mercury measurements.

Both denuders and CEMs have limitations in retaining Hg^{II} during the pre-concentration process. However, this study confirmed that CEM-based measurements exhibit significantly lower losses of Hg^{II} compounds compared to denuders, consistent with previous findings. While earlier studies have shown that CEMs typically yield higher Hg^{II} measurements than denuders, it is important to acknowledge that CEMs may not uniformly collect all Hg^{II} species with equal efficiency. Nevertheless, their superior performance in retaining ionic Hg^{II} species, such as mercury chloride and bromide—predominant in the atmosphere—underscores their potential suitability for more accurate Hg^{II} measurement. Nonetheless, in the presence of neutral species such as HgO , CEMs may not be the optimal sampling method as losses can be significant. The $^{197}\text{Hg}^{\text{II}}$ mass distribution within the CEM filter pack cartridge demonstrated that not all Hg^{II} sampled from the air is necessarily captured on the CEM, a small amount (6.2% on average) can also be captured on the inner Teflon parts of the filter pack cartridge. Therefore, careful consideration has to be made for recovering all Hg^{II} sampled by this method, in order to minimize additional biases that may arise due to sample treatment, beyond those from pre-concentration.

Debates within the scientific community continue regarding the potential phasing out of denuder for Hg^{II} measurements. However, it is essential to recognize that both denuders and CEMs each have unique strengths and limitations. We suggest that with proper calibration approaches, Tekran/1130 denuder-based Hg^{II} measurements in conjunction with CEMs can still be used to monitor trends in atmospheric Hg concentrations, leveraging the high time resolution of denuders, which CEM measurements lack. When properly calibrated and with measurement uncertainties carefully accounted for, data from both systems can provide equivalent results. However, biases must be quantified and reported accurately. Quantifying biases along with considering other ambient factors could help in correcting historical Hg^{II} /RM data to some extent. Future studies evaluating model outputs against available Hg observation data should account for measurement biases to improve the accuracy and reliability of the model findings.

This study suggests a shift toward CEM-based methods, but optimizing digestion, calibration, and validation protocols is crucial to ensure accurate long-term Hg monitoring. Future research should focus on refining sample recovery, improving calibration traceability, and validating measurements under diverse atmospheric conditions.

Supplement

The supplementary material related to this article is available online at:

Data availability

Data will be available from the corresponding author upon reasonable request.

Author contribution

SVN: Writing—original draft, Conceptualization, Methodology, Data curation, Investigation, Formal analysis, Visualization, Writing—review and editing. SWA: Investigation, Writing—review and editing. JG: Methodology, Investigation, Writing—review and editing. IŽ: Methodology, Validation, Writing—review and editing. TA: Investigation, Writing—review and editing.



OT: Methodology, Validation, Writing—review and editing. MH: Conceptualization, Methodology, Validation, Resources, Funding acquisition, Writing—review and editing, Supervision, Project administration.

Competing interests

335 The authors declare that they have no conflict of interest.

Acknowledgement

The authors thank to the Metrology Institute of the Republic of Slovenia (MIRS) under contract No. C2182-25-000016 (6401-1/2024/41) for activities and obligations performed as a Designate Institute.

340 Financial support

This research work was part of the GMOS-Train project funded by European Union's Horizon 2020 research and innovation programme under the Marie Skłodowska-Curie grant agreement no. 860497. The research has also been co-funded by the SI-Hg project under the European Metrology Programme for Innovation and Research (EMPIR; grant agreement no. 19NRM03), Slovenian Research and Innovation Agency (ARIS) programme P1-0143, and projects J1-1716 (STRAP) and J1-3033 (IsoCont).

345

References

Ali, S. W., Božič, D., Vijayakumaran Nair, S., Živković, I., Gačnik, J., Andron, T.-D., Jagodic Hudobivnik, M., Kocman, D., and Horvat, M.: Optimization of a pre-concentration method for the analysis of mercury isotopes in low-concentration foliar samples, *Anal. Bioanal. Chem.*, 416, 1239–1248, <https://doi.org/10.1007/s00216-023-05116-5>, 2024.

350 Ariya, P. A., Amyot, M., Dastoor, A., Deeds, D., Feinberg, A., Kos, G., Poulain, A., Ryjkov, A., Semeniuk, K., Subir, M., and Toyota, K.: Mercury Physicochemical and Biogeochemical Transformation in the Atmosphere and at Atmospheric Interfaces: A Review and Future Directions, *Chem. Rev.*, 115, 3760–3802, <https://doi.org/10.1021/cr500667e>, 2015.

Cheng, I. and Zhang, L.: Uncertainty Assessment of Gaseous Oxidized Mercury Measurements Collected by Atmospheric Mercury Network, *Environ. Sci. Technol.*, 51, 855–862, <https://doi.org/10.1021/acs.est.6b04926>, 2017.

355 Dastoor, A., Wilson, S. J., Travníkov, O., Ryjkov, A., Angot, H., Christensen, J. H., Steenhuisen, F., and Muntean, M.: Arctic atmospheric mercury: Sources and changes, *Sci. Total Environ.*, 839, 156213, <https://doi.org/10.1016/j.scitotenv.2022.156213>, 2022.

Davis, M. and Lu, J.: Calibration Sources for Gaseous Oxidized Mercury: A Review of Source Design, Performance, and Operational Parameters, *Crit. Rev. Anal. Chem.*, 1–10, <https://doi.org/10.1080/10408347.2022.2131373>, 2022.

360 Driscoll, C. T., Mason, R. P., Chan, H. M., Jacob, D. J., and Pirrone, N.: Mercury as a Global Pollutant: Sources, Pathways, and Effects, *Environ. Sci. Technol.*, 47, 4967–4983, <https://doi.org/10.1021/es305071v>, 2013.

Dunham-Cheatham, S. M., Lyman, S., and Gustin, M. S.: Comparison and calibration of methods for ambient reactive mercury quantification, *Sci. Total Environ.*, 856, 159219, <https://doi.org/10.1016/j.scitotenv.2022.159219>, 2023.

365 Elgiar, T. R., Lyman, S. N., Andron, T. D., Gratz, L., Hallar, A. G., Horvat, M., Vijayakumaran Nair, S., O'Neil, T., Volkamer, R., and Živković, I.: Traceable Calibration of Atmospheric Oxidized Mercury Measurements, *Environ. Sci. Technol.*, 58, 10706–10716, <https://doi.org/10.1021/acs.est.4c02209>, 2024.

EMEP: EMEP Status Report: Assessment of transboundary pollution with heavy metals and POPs, 2024.

Feng, X., Lu, J. Y., Hao, Y., Banic, C., and Schroeder, W. H.: Evaluation and applications of a gaseous mercuric chloride source, *Anal. Bioanal. Chem.*, 376, 1137–1140, <https://doi.org/10.1007/s00216-003-2034-7>, 2003.



- 370 Gačnik, J., Živković, I., Ribeiro Guevara, S., Jaćimović, R., Kotnik, J., De Feo, G., Dexter, M. A., Corns, W. T., and Horvat, M.: Behavior of KCl sorbent traps and KCl trapping solutions used for atmospheric mercury speciation: stability and specificity, *Atmospheric Meas. Tech.*, 14, 6619–6631, <https://doi.org/10.5194/amt-14-6619-2021>, 2021a.
- Gačnik, J., Živković, I., Ribeiro Guevara, S., Jaćimović, R., Kotnik, J., and Horvat, M.: Validating an Evaporative Calibrator for Gaseous Oxidized Mercury, *Sensors*, 21, 2501, <https://doi.org/10.3390/s21072501>, 2021b.
- 375 Gačnik, J., Živković, I., Ribeiro Guevara, S., Kotnik, J., Berisha, S., Vijayakumaran Nair, S., Jurov, A., Cvelbar, U., and Horvat, M.: Calibration Approach for Gaseous Oxidized Mercury Based on Nonthermal Plasma Oxidation of Elemental Mercury, *Anal. Chem.*, *acs.analchem.2c00260*, <https://doi.org/10.1021/acs.analchem.2c00260>, 2022a.
- Gačnik, J., Živković, I., Ribeiro Guevara, S., Kotnik, J., Berisha, S., Vijayakumaran Nair, S., Jurov, A., Cvelbar, U., and Horvat, M.: Calibration Approach for Gaseous Oxidized Mercury Based on Nonthermal Plasma Oxidation of Elemental Mercury, *Anal. Chem.*, 94, 8234–8240, <https://doi.org/10.1021/acs.analchem.2c00260>, 2022b.
- 380 Gonzalez-Raymat, H., Liu, G., Liriano, C., Li, Y., Yin, Y., Shi, J., Jiang, G., and Cai, Y.: Elemental mercury: Its unique properties affect its behavior and fate in the environment, *Environ. Pollut.*, 229, 69–86, <https://doi.org/10.1016/j.envpol.2017.04.101>, 2017.
- Gustin, M. and Jaffe, D.: Reducing the Uncertainty in Measurement and Understanding of Mercury in the Atmosphere, *Environ. Sci. Technol.*, 44, 2222–2227, <https://doi.org/10.1021/es902736k>, 2010.
- 385 Gustin, M. S., Amos, H. M., Huang, J., Miller, M. B., and Heidecorn, K.: Measuring and modeling mercury in the atmosphere: a critical review, *Atmospheric Chem. Phys.*, 15, 5697–5713, <https://doi.org/10.5194/acp-15-5697-2015>, 2015.
- Gustin, M. S., Dunham-Cheatham, S. M., and Zhang, L.: Comparison of 4 Methods for Measurement of Reactive, Gaseous Oxidized, and Particulate Bound Mercury, *Environ. Sci. Technol.*, 53, 14489–14495, <https://doi.org/10.1021/acs.est.9b04648>, 2019.
- 390 Gustin, M. S., Dunham-Cheatham, S. M., Lyman, S., Horvat, M., Gay, D. A., Gačnik, J., Gratz, L., Kempkes, G., Khalizov, A., Lin, C.-J., Lindberg, S. E., Lown, L., Martin, L., Mason, R. P., MacSween, K., Vijayakumaran Nair, S., Nguyen, L. S. P., O’Neil, T., Sommar, J., Weiss-Penzias, P., Zhang, L., and Živković, I.: Measurement of Atmospheric Mercury: Current Limitations and Suggestions for Paths Forward, *Environ. Sci. Technol.*, 58, 12853–12864, <https://doi.org/10.1021/acs.est.4c06011>, 2024.
- Huang, J. and Gustin, M. S.: Uncertainties of Gaseous Oxidized Mercury Measurements Using KCl-Coated Denuders, Cation-Exchange Membranes, and Nylon Membranes: Humidity Influences, *Environ. Sci. Technol.*, 49, 6102–6108, <https://doi.org/10.1021/acs.est.5b00098>, 2015.
- 395 Huang, J., Miller, M. B., Weiss-Penzias, P., and Gustin, M. S.: Comparison of Gaseous Oxidized Hg Measured by KCl-Coated Denuders, and Nylon and Cation Exchange Membranes, *Environ. Sci. Technol.*, 47, 7307–7316, <https://doi.org/10.1021/es4012349>, 2013.
- 400 Huang, J., Miller, M. B., Edgerton, E., and Sexauer Gustin, M.: Deciphering potential chemical compounds of gaseous oxidized mercury in Florida, USA, *Atmospheric Chem. Phys.*, 17, 1689–1698, <https://doi.org/10.5194/acp-17-1689-2017>, 2017.
- Jaffe, D. A., Lyman, S., Amos, H. M., Gustin, M. S., Huang, J., Selin, N. E., Levin, L., ter Schure, A., Mason, R. P., Talbot, R., Rutter, A., Finley, B., Jaeglé, L., Shah, V., McClure, C., Ambrose, J., Gratz, L., Lindberg, S., Weiss-Penzias, P., Sheu, G.-R., Feddersen, D., Horvat, M., Dastoor, A., Hynes, A. J., Mao, H., Sonke, J. E., Slemr, F., Fisher, J. A., Ebinghaus, R., Zhang, Y., and Edwards, G.: Progress on Understanding Atmospheric Mercury Hampered by Uncertain Measurements, *Environ. Sci. Technol.*, 48, 7204–7206, <https://doi.org/10.1021/es5026432>, 2014.
- 405 Kocman, D., Horvat, M., Pirrone, N., and Cinnirella, S.: Contribution of contaminated sites to the global mercury budget, *Environ. Res.*, 125, 160–170, <https://doi.org/10.1016/j.envres.2012.12.011>, 2013.
- Landis, M. S., Stevens, R. K., Schaedlich, F., and Prestbo, E. M.: Development and Characterization of an Annular Denuder Methodology for the Measurement of Divalent Inorganic Reactive Gaseous Mercury in Ambient Air, *Environ. Sci. Technol.*, 36, 3000–3009, <https://doi.org/10.1021/es015887t>, 2002.
- Luippold, A., Gustin, M. S., Dunham-Cheatham, S. M., and Zhang, L.: Improvement of quantification and identification of atmospheric reactive mercury, *Atmos. Environ.*, 224, 117307, <https://doi.org/10.1016/j.atmosenv.2020.117307>, 2020.



- 415 Lyman, S., Jones, C., O'Neil, T., Allen, T., Miller, M., Gustin, M. S., Pierce, A. M., Luke, W., Ren, X., and Kelley, P.: Automated Calibration of Atmospheric Oxidized Mercury Measurements, *Environ. Sci. Technol.*, 50, 12921–12927, <https://doi.org/10.1021/acs.est.6b04211>, 2016.
- Lyman, S. N., Jaffe, D. A., and Gustin, M. S.: Release of mercury halides from KCl denuders in the presence of ozone, *Atmospheric Chem. Phys.*, 10, 8197–8204, <https://doi.org/10.5194/acp-10-8197-2010>, 2010.
- 420 Lyman, S. N., Cheng, I., Gratz, L. E., Weiss-Penzias, P., and Zhang, L.: An updated review of atmospheric mercury, *Sci. Total Environ.*, 707, 135575, <https://doi.org/10.1016/j.scitotenv.2019.135575>, 2020a.
- Lyman, S. N., Gratz, L. E., Dunham-Cheatham, S. M., Gustin, M. S., and Luippold, A.: Improvements to the Accuracy of Atmospheric Oxidized Mercury Measurements, *Environ. Sci. Technol.*, 54, 13379–13388, <https://doi.org/10.1021/acs.est.0c02747>, 2020b.
- 425 Maruszczak, N., Sonke, J. E., Fu, X., and Jiskra, M.: Tropospheric GOM at the Pic du Midi Observatory—Correcting Bias in Denuder Based Observations, *Environ. Sci. Technol.*, 51, 863–869, <https://doi.org/10.1021/acs.est.6b04999>, 2017.
- McClure, C. D., Jaffe, D. A., and Edgerton, E. S.: Evaluation of the KCl Denuder Method for Gaseous Oxidized Mercury using HgBr₂ at an In-Service AMNet Site, *Environ. Sci. Technol.*, 48, 11437–11444, <https://doi.org/10.1021/es502545k>, 2014.
- 430 Miller, M. B., Dunham-Cheatham, S. M., Gustin, M. S., and Edwards, G. C.: Evaluation of cation exchange membrane performance under exposure to high Hg⁰ and HgBr₂ concentrations, *Atmospheric Meas. Tech.*, 12, 1207–1217, <https://doi.org/10.5194/amt-12-1207-2019>, 2019.
- Outridge, P. M., Mason, R. P., Wang, F., Guerrero, S., and Heimbürger-Boavida, L. E.: Updated Global and Oceanic Mercury Budgets for the United Nations Global Mercury Assessment 2018, *Environ. Sci. Technol.*, 52, 11466–11477, <https://doi.org/10.1021/acs.est.8b01246>, 2018.
- 435 Pacyna, E. G., Pacyna, J. M., Steenhuisen, F., and Wilson, S.: Global anthropogenic mercury emission inventory for 2000, *Atmos. Environ.*, 40, 4048–4063, <https://doi.org/10.1016/j.atmosenv.2006.03.041>, 2006.
- Peter Mason, R., Amouroux, D., Chen, J., and Dastoor, A.: Environmental chemistry of mercury: Sources, pathways, transformations and impact, *Frontiers Media SA*, <https://doi.org/10.3389/978-2-8325-4368-9>, 2024.
- 440 Pirrone, N., Cinnirella, S., Feng, X., Finkelman, R. B., Friedli, H. R., Leaner, J., Mason, R., Mukherjee, A. B., Stracher, G., Streets, D. G., and Telmer, K.: Global Mercury Emissions to the Atmosphere from Natural and Anthropogenic Sources, in: *Mercury Fate and Transport in the Global Atmosphere: Emissions, Measurements and Models*, edited by: Mason, R. and Pirrone, N., Springer US, Boston, MA, 1–47, https://doi.org/10.1007/978-0-387-93958-2_1, 2009.
- Ribeiro Guevara, S., Žižek, S., Repinc, U., Pérez Catán, S., Jaćimović, R., and Horvat, M.: Novel methodology for the study of mercury methylation and reduction in sediments and water using 197Hg radiotracer, *Anal. Bioanal. Chem.*, 387, 2185–2197, <https://doi.org/10.1007/s00216-006-1040-y>, 2007.
- 445 Ryaboshapko, A., Bullock, R., Ebinghaus, R., Ilyin, I., Lohman, K., Munthe, J., Petersen, G., Seigneur, C., and Wängberg, I.: Comparison of mercury chemistry models, *Atmos. Environ.*, 36, 3881–3898, [https://doi.org/10.1016/S1352-2310\(02\)00351-5](https://doi.org/10.1016/S1352-2310(02)00351-5), 2002.
- Sandström, M., Persson, I., and Persson, P.: A Study of Solvent Electron-Pair Donor Ability and Lewis Basicity Scales, *Acta Chem. Scand.*, 44, 1990.
- 450 Sari, S., Timo, R., Jussi, H., and Panu, H.: Dynamic calibration method for reactive gases, *Meas. Sci. Technol.*, 31, 034001, <https://doi.org/10.1088/1361-6501/ab4d68>, 2020.
- Schroeder, W. H. and Munthe, J.: Atmospheric mercury—An overview, *Atmos. Environ.*, 32, 809–822, [https://doi.org/10.1016/S1352-2310\(97\)00293-8](https://doi.org/10.1016/S1352-2310(97)00293-8), 1998.
- 455 Selin, N. E.: Global Biogeochemical Cycling of Mercury: A Review, *Annu. Rev. Environ. Resour.*, 34, 43–63, <https://doi.org/10.1146/annurev.enviro.051308.084314>, 2009.



Si, L. and Ariya, P.: Recent Advances in Atmospheric Chemistry of Mercury, *Atmosphere*, 9, 76, <https://doi.org/10.3390/atmos9020076>, 2018.

Smirnova, S. V., Ilin, D. V., and Pletnev, I. V.: Extraction and ICP-OES determination of heavy metals using tetrabutylammonium bromide aqueous biphasic system and oleophilic collector, *Talanta*, 221, 121485, <https://doi.org/10.1016/j.talanta.2020.121485>, 2021.

Travnikov, O., Angot, H., Artaxo, P., Bencardino, M., Bieser, J., D'Amore, F., Dastoor, A., De Simone, F., Diéguez, M. D. C., Dommergue, A., Ebinghaus, R., Feng, X. B., Gencarelli, C. N., Hedgecock, I. M., Magand, O., Martin, L., Matthias, V., Mashyanov, N., Pirrone, N., Ramachandran, R., Read, K. A., Ryjkov, A., Selin, N. E., Sena, F., Song, S., Sprovieri, F., Wip, D., Wängberg, I., and Yang, X.: Multi-model study of mercury dispersion in the atmosphere: atmospheric processes and model evaluation, *Atmospheric Chem. Phys.*, 17, 5271–5295, <https://doi.org/10.5194/acp-17-5271-2017>, 2017.

Travnikov, O., Gačnik, J., Vijayakumaran Nair, S., Živković, I., Horvat, M., Sprovieri, F., Tassone, A., and Pirrone, N.: Use of corrected reactive mercury measurements for model evaluation: Analysis and implications for global model estimates, 2024.

UNEP: GUIDANCE ON MONITORING OF MERCURY AND MERCURY COMPOUNDS TO SUPPORT EVALUATION OF THE EFFECTIVENESS OF THE MINAMATA CONVENTION, 2021.

Vijayakumaran Nair, S., Gačnik, J., Živković, I., Andron, T. D., Ali, S. W., Kotnik, J., and Horvat, M.: Application of traceable calibration for gaseous oxidized mercury in air, *Anal. Chim. Acta*, 1288, 342168, <https://doi.org/10.1016/j.aca.2023.342168>, 2024.

Xu, L., Chen, J., Niu, Z., Yin, L., and Chen, Y.: Characterization of mercury in atmospheric particulate matter in the southeast coastal cities of China, *Atmospheric Pollut. Res.*, 4, 454–461, <https://doi.org/10.5094/APR.2013.052>, 2013.

Zhang, H., Fu, X., Yu, B., Li, B., Liu, P., Zhang, G., Zhang, L., and Feng, X.: Speciated atmospheric mercury at the Waliguan Global Atmosphere Watch station in the northeastern Tibetan Plateau: implication of dust-related sources for particulate bound mercury, *Atmospheric Chem. Phys.*, 21, 15847–15859, <https://doi.org/10.5194/acp-21-15847-2021>, 2021.

Zhang, X., Siddiqi, Z., Song, X., Mandiwana, K. L., Yousaf, M., and Lu, J.: Atmospheric dry and wet deposition of mercury in Toronto, *Atmos. Environ.*, 50, 60–65, <https://doi.org/10.1016/j.atmosenv.2011.12.062>, 2012.